Asia-Pacific Journal of Science and Technology :Volume :27 .Issue :01 .Article ID :.APST-27-01-04. Research Article

APST

Asia-Pacific Journal of Science and Technology

https//:www.tci-thaijo.org/index.php/APST/index

Published by the Research and Graduate Studies,
Khon Kaen University, Thailand

The design and analysis of low-cost myoelectric hand using six-bar linkage mechanism

Rifky Ismail[1,2,*], Mochammad Ariyanto[1,2], Luthfi R. Wicaksono[2], Aditya Ispramuditya[2] and Farika T. Putri[3]

[1]Center for Biomechanics, Biomaterial, Biomechatronics and Biosignal Processing (CBIOM3S), Diponegoro University, Semarang, Indonesia
[2]Department of Mechanical Engineering, Diponegoro University, Semarang, Indonesia
[3]Mechanical Engineering Department, Semarang State Polytechnic, Semarang, Indonesia
[*]Corresponding author: rifky_ismail@ft.undip.ac.id

Received 14 July 2020
Revised 25 January 2021
Accepted 29 January 2021

Abstract

This study discussed the development of an affordable myoelectric prosthetic hand using a six-bar linkage. This involved the design of the index, middle, ring, and little finger using computer-aided design software with the application of two six-bar linkages as the main mechanism. The fingertip trajectories were also simulated using the software before the hand prototype was built after which they were analyzed based on six-bar linkage using the trigonometric law. Moreover, the hand design was developed using 3D printing technology while six grip patterns were implemented to ensure the hand performs the required daily activities, and individual grip force for each finger was measured using a calibrated force-sensitive resistor. The experimental results showed the designed six grip patterns successfully pick and grasp several objects with different weights, shapes, and sizes. The proposed BimoHand has individual grip force at the fingertip ranging from 0.5886 N to 1.373 N and also successfully gripped and handle a fragile object such as an egg by adjusting the human hand flexion and extension without breaking it. It has a total mass of 251 grams excluding socket hand and batteries and this lightweight makes it comfortable and easy to use in daily activities. The hand is relatively affordable and lighter compared to other available myoelectric hands.

Keywords: Low-cost, Prosthetic hand, Four-bar linkage, Mechanism

1. Introduction

Nomenclature

A	Position of point A in (x, y) coordinate (mm)
B	Position of point B in (x, y) coordinate (mm)
X_D	Position of point D in the x-axis (mm)
Y_D	Position of point D in the y-axis (mm)
X_E	Position of point E in the y-axis (mm)
Y_E	Position of point E in the y-axis (mm)
a	Length link of link AO_1 in closed-loop six-bar linkage (mm)
b	Length link of link BO_2 in closed-loop six-bar linkage (mm)
c	Length link of link O_2D in closed-loop six-bar linkage (mm)
d	Length link of link O_3C in closed-loop six-bar linkage (mm)
e	Distance from O_3 to D (mm)
g	Length link of link O_1O_2 in closed-loop six-bar linkage (mm)
h	Length link of link AB in closed-loop six-bar linkage (mm)
i	Length link of link O_2O_3 in closed-loop six-bar linkage (mm)
j	Length link of link CD in closed-loop six-bar linkage (mm)
α	Angle of O_3O_2D in closed-loop six-bar linkage in finger mechanism (degree)
β	Angle of CD O_2 in closed-loop six-bar linkage in finger mechanism (degree)
γ	Angle of link O_2D with respect to the horizontal axis (degree)
φ	Angle of link DE with respect to the link O_2D (degree)
θ	Angle of AO_1O_2 in closed-loop six-bar linkage in finger mechanism (degree)
ψ	Angle of BO_2D in closed-loop six-bar linkage in finger mechanism (degree)

The need for an active prosthetic hand such as a myoelectric prosthetic hand is increasing in developing and underdeveloped countries. This is due to the occurrence of trans-radial amputation mostly through work accidents or trauma from road accidents and even, in some cases, some are born without hands. Several people in developing countries do not have sufficient economic strength to buy a myoelectric hand due to its quite expensive. This has, therefore, led to the utilization of conventional steel hook prostheses, passive prosthetic hand, and body-powered prosthetic hand by trans-radial amputees. These people also wear cosmetic prosthetic hand which makes it impossible for them to move it to do daily activities. Therefore, researchers have started developing affordable myoelectric prosthetic hands which are easy to maintain or repair, have the same size as the human hand, and have lightweight. The use of 3D printing technology has also been proposed for the production of these prosthetic hands due to the availability of cheap materials during the manufacturing stage.

Myoelectric prosthetic hands have been studied by some universities such as AstoHand [1,2], Tact [3], Rehand [4], Smart Hand [5,6], and Keio Hand [7]. The focus is on [1-4] affordability [5,7] and achieving the complexity of dynamics and control as observed in open-sources of low-cost prosthetic hands such as Ada Hand [8], Brunel and Dextrus [9], and Exiii Hackberry [10] designed to ensure more lightweight and affordability.

The high-end products currently being sold in the market include Vincent Hand [11], Michelangelo [12], Bebionic [13], and iLimb [14] and they have more performance and durability compared to low-cost products but are expensive and unaffordable to several people, especially in developing countries. Most of their parts are also produced using metal or carbon fiber.

The joint couple method most widely used for open-source low-cost prosthetic hands [8,9] is the tendon mechanism with a DC motor applied as the actuator. This mechanism enables the fingers to comply and mimic the human fingers. Meanwhile, Tact and Exiii Hackberry use linkage from the actuators to the fingers and this is beneficial due to its more precise and accurate motion but its design is very challenging. Another type of joint couple method in the hand finger mechanism is twisted string actuation and this converts angular to linear motion in order to produce high contraction force [15-17].

This study, therefore, aimed to produce a lightweight and low-cost myoelectric prosthetic hand through the use of a six-bar linkage as the joint couple method in four fingers as observed in previous studies [18-19]. A 3D printing technology was also applied in the production of this hand which was designed to use four servo motors and one DC motor as the actuators. Moreover, the two six-bar linkages applied as the joint couple method in the index, middle, ring, and little fingers were designed and analyzed using the trigonometric approach with their trajectories and input presented. The prosthetic hand was tested for grasping ability using different objects after it has been assembled and the force generated by each finger was measured using a force-sensitive resistor (FSR). The hand was also used to grasp a fragile object like an egg without force feedback control.

2. Materials and methods

2.1 Underactuated finger and thumb design

2.1.1 Finger design and analysis

A myoelectric hand which used four servo motors and one DC motor as the main actuator was proposed in this study. Meanwhile, a microcontroller unit (MCU) and other electronic components as well as four metal gear micro servo motors were selected to drive the finger mechanism due to the limited space for actuators in the hand. This involved using two micro servo motors to drive the index and middle fingers while one was used for the ring and little fingers and the last serve as the linkage to couple the ring and little finger together. It is important to note that the index, middle, ring, and little fingers were designed for one degree of freedom (DOF) which includes the flexion and extension motion while the thumb was for two DOF including the flexion or extension and opposition or reposition motion.

The final finger design in the 3D model is presented in Figure 1. The distal interphalangeal (DIP) joint was set with a fixed angle of 15 degrees for the two DOF finger designs as shown in Figure 1A while the metacarpophalangeal (MCP) and proximal interphalangeal (PIP) joints can be rotated from 0 degrees to 90 degrees as shown in Figure 1b. All the finger mechanisms are, however, linked to the servo motor through two six-bar linkages.

All the mechatronics components were selected to fit into the proposed hand in order to have the same or smaller size as the average natural human hand. Figure 2 shows how the four micro servo motors and other components are placed in the palm as well as the LED and tactile switch placed on the back cover. Meanwhile, the battery and electromyography (EMG) sensor are placed in the socket.

(A) (B)

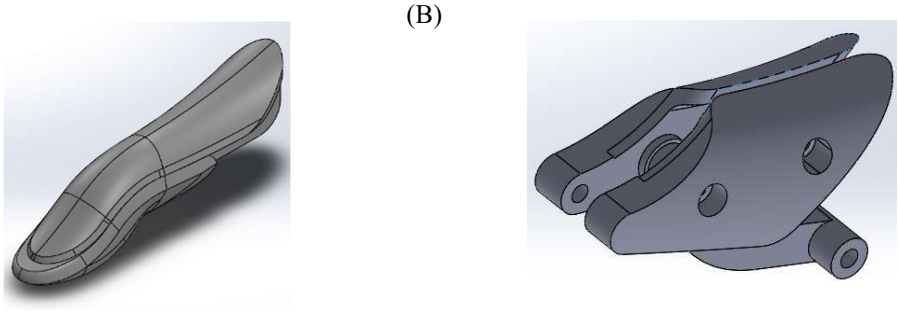

Figure 1 3D model design: (A) Distal-medial with fixed DIP joint (B) Proximal with MCP and PIP joints.

(A) (B)

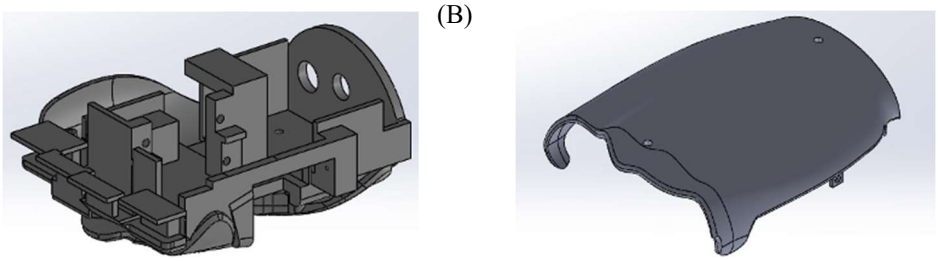

Figure 2 3D model for the palm and back cover (A) Palm (B) Back cover.

(A) (B)

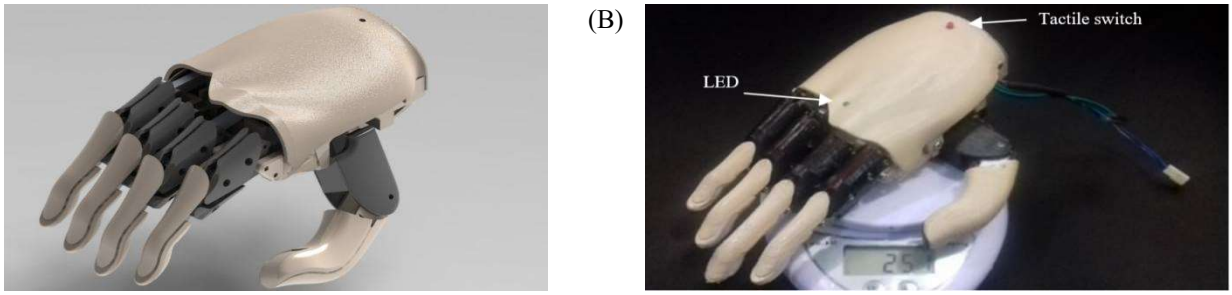

Figure 3 The proposed myoelectric prosthetic hand: (A) 3D model (B) Assembled prosthetic hand.

The final design and assembled myoelectric hand components are presented in Figure 3. The 3D design presented in Figure 3a was developed using SolidWorks software selected due to its motion study feature which is useful to simulate the motion in the four-bar linkage. Moreover, two six-bar linkages were employed to construct the four-finger mechanisms including the index, middle, ring, and little fingers as shown in Figure 4. The linkages have three fixed-points O_1, O_2, and O_3, and their analysis is divided into loop O_1ABO_2, and loop O_2O_3CD with the link O_1O_2 and link O_2O_3 fixed at a length of g and i respectively. The two six-bar linkages have one degree of freedom (DOF) with an input angle θ and an output angle β as shown in Figure 4.

Sine and cosine law was employed to calculate the movement of the linkage position on point A and point B of the finger linkage in the six-bar mechanism. As presented in Figure 5, the angle θ or crank angle is the angle formed between the servo motor link AO_2 with the ground frame O_1O_2 with a length of g mm. Moreover, the servo motor link AO_2 has a mm length which was assumed as the input or crank link, and connected to link coupler AB which has long h mm. This coupler was used to connect the input link with the output or rocker link BO_2 which has a length of b mm. Meanwhile, the angle ψ is the angle formed between the link O1O2 and BO2 as shown in Figure 5.

(A) (B)

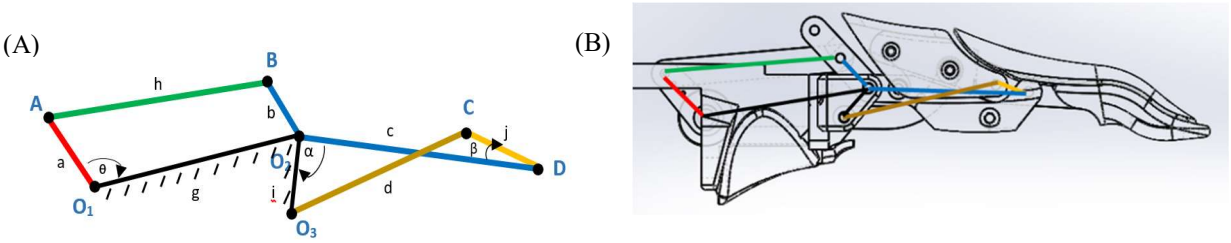

Figure 4 Two six-bar linkages in finger mechanism: (A) Six-bar linkage in finger mechanism (B) Schematic of two six-bar linkages.

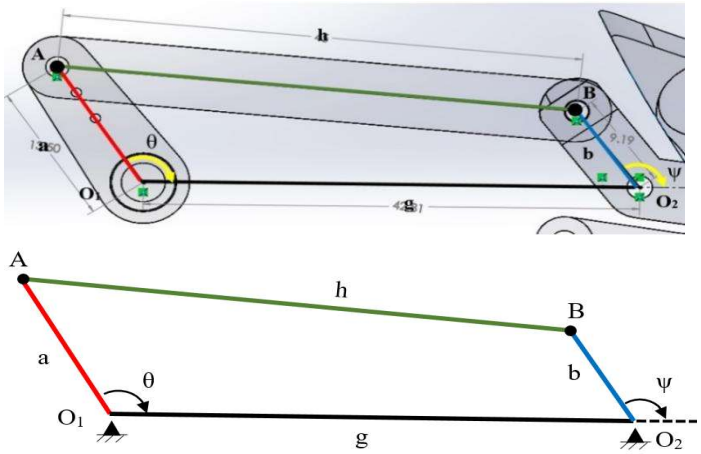

Figure 5 Closed-loop six-bar linkage in finger mechanism.

Figure 5 shows the position of point A and point B in (x, y) coordinate as expressed in equation (1)

$$\begin{bmatrix} A_x \\ A_y \end{bmatrix} = \begin{bmatrix} a\cos\theta \\ a\sin\theta \end{bmatrix}; and \quad \begin{bmatrix} B_x \\ B_y \end{bmatrix} = \begin{bmatrix} g + b\cos\psi \\ b\sin\psi \end{bmatrix} \tag{1}$$

The length of the link connecting points A and B is fixed at h while the value for each link in index, middle, ring, and little fingers is summarized in Table I. The constraint equation was calculated using Equations (2), (3), and (4) as follows.

$$(g + b\cos\psi - a\cos\theta)^2 + (b\sin\psi - a\sin\theta)^2 = h^2 \tag{2}$$

$$g^2 - 2ag\cos\theta + 2bg\cos\psi - ab\cos\theta\cos\psi + a^2 + b^2 - 2ab\sin\theta\sin\psi = h^2 \tag{3}$$

$$(2bg - ab\cos\theta)\cos\psi - (2ab\sin\theta)\sin\psi = h^2 - g^2 - a^2 - b^2 + 2ag\cos\theta \tag{4}$$

It is, however, possible to group Equation (4) into cos ψ and sin ψ to produce a general form as shown in Equation (5).

$$\lambda(\theta)\cos\psi + \sigma(\theta)\sin\psi = \zeta(\theta) \tag{5}$$

Where

$$\lambda(\theta) = 2bg - 2ab\cos\theta \tag{6}$$

$$\sigma(\theta) = -2ab\sin\theta \tag{7}$$

$$\zeta(\theta) = h^2 - g^2 - b^2 - a^2 + 2ag\cos\theta \tag{8}$$

The variable ψ can be expressed as a function of θ by dividing the three segments in Equation (5) with $\sqrt{\lambda^2 + \sigma^2}$ to obtain the following equation as in (9)

$$\frac{\lambda}{\sqrt{\lambda^2 + \sigma^2}}\cos\psi + \frac{\sigma}{\sqrt{\lambda^2 + \sigma^2}}\sin\psi = \frac{\zeta}{\sqrt{\lambda^2 + \sigma^2}} \tag{9}$$

The final equation to determine the variable ψ in Equation (10) can be calculated by utilizing Equation (11)

$$\cos\phi = \frac{\lambda}{\sqrt{\lambda^2+\sigma^2}}, \sin\phi = \frac{\sigma}{\sqrt{\lambda^2+\sigma^2}}, \phi = \tan^{-1}\left(\frac{\sigma}{\lambda}\right) \tag{10}$$

$$\psi = \tan^{-1}\left(\frac{\sigma}{\lambda}\right) \pm \cos^{-1}\left(\frac{\zeta}{\sqrt{\lambda^2+\sigma^2}}\right) \tag{11}$$

Table 1 Lengths of the links for the six-bar linkage on four fingers.

Fingers	a (mm)	b (mm)	g (mm)	h (mm)	θ (deg)
Index	13.5	9.19	42.81	45	65-125
Middle	10.5	9.19	49.52	45	20-110
Ring	13.5	9.19	56.74	50	5-85
Little	13.5	9.19	56.74	50	5-85

Cosine law can be used to determine the movement of the linkage position radius in the crossed six-bar mechanism. The input angle α is the angle formed between the proximal linkage O_2D with a length of c mm and a medial linkage O_2O_3 with a length of i mm which is connected to a distal link CD with a length of j mm as shown in Figure 6. The movement of the distal link CD is, however, influenced by medial2 links O3C with a length of d mm. Meanwhile, angle β was calculated using equation (12) while the angle of $<O_3DC$ and $<O_2DO_3$ was determined using Equations (13) and (14) and the value of e computed using Equation (15).

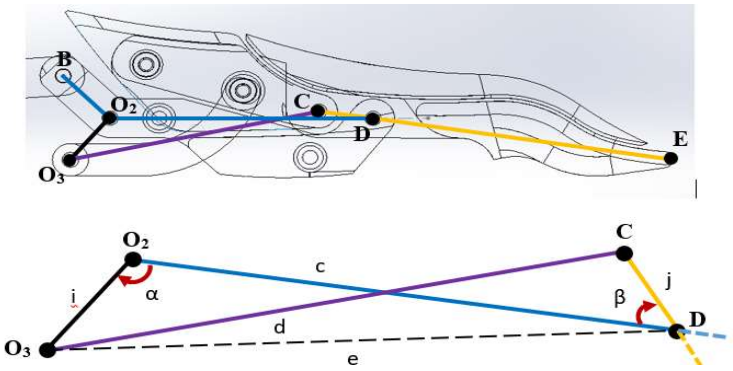

Figure 6 Crossed closed-loop six-bar linkage in the finger mechanism.

$$\beta = \angle O_3DC - \angle O_2DO_3 \tag{12}$$

$$\angle O_3DC = \cos^{-1}\left(\frac{e^2+j^2-d^2}{2ej}\right) \tag{13}$$

$$\angle O_2DO_3 = \cos^{-1}\left(\frac{c^2+e^2-i^2}{2ce}\right) \tag{14}$$

$$e = \sqrt{c^2+i^2-2ci\cos\alpha} \tag{15}$$

The two links O_2D and DE presented in Figure 7 were employed to calculate the trajectory of the fingers. The O_2D link was, however, observed to have an angle γ while the CD link has φ.

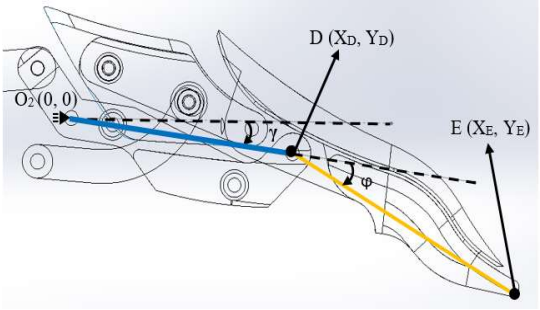

Figure 7 Link configuration on a finger.

The angles for α and β obtained were used to simulate the movement of each finger using the link configurations presented in Figure 7 which focuses on fingertips. Link O_2D is illustrated using a blue line while CD is with a yellow line. The initial angle of γ is 0^0 and the initial angle φ is 9^0. The position of point D on the base palm was determined using Equation (16) while the position of point E used Equation (17). The other parameters in Figure 7 are, however, summarized in Table II.

$$\begin{aligned} X_D &= l_1 \cos\gamma \\ Y_D &= l_1 \sin\gamma \\ \gamma &= 130^o - \alpha \end{aligned} \tag{16}$$

$$\begin{aligned} X_E &= l_2 \cos(\gamma+\beta) + l_1 \cos\gamma \\ Y_E &= l_2 \sin(\gamma+\beta) + l_1 \sin\gamma \end{aligned} \tag{17}$$

Table 2 Length of the two links on the fingers.

Fingers	γ (deg)	Link O_2D (mm)	Link DE (mm)
Index	0-90	36.4	41.84
Middle	0-90	36.4	45.63
Ring	0-90	36.4	41.84
Little	0-90	36.4	37.27

The thumb was designed using a metal gear servo motor for the opposition or reposition in the carpometacarpal (CMC) joint and a DC motor for the flexion or extension in the metacarpophalangeal (MP) joint. The motion of the opposition or reposition was through the worm and spur gears with the CMC joint observed to have an important role in opposing grasp motion, especially in the thumb pinch and power grip. The 3D design of the thumb is presented in Figure 8 and the two DOF of thumb motion are described in Figure 9 while the placement of the servomotor, DC motor, and gear joint is shown in Figure 10.

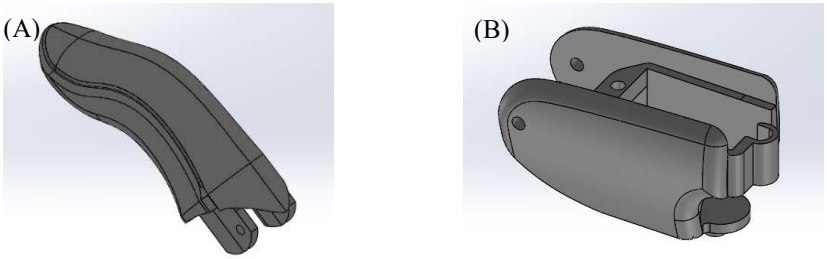

Figure 8 3D thumb design: (A) Distal phalanx and proximal phalanx (B) Metacarpal.

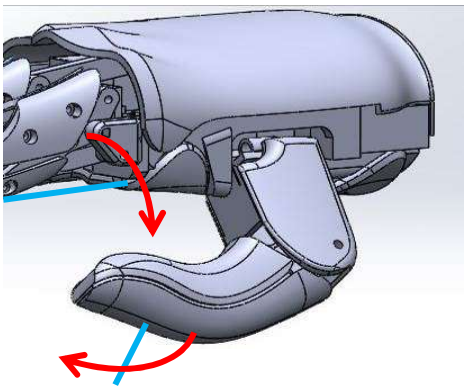

Figure 9 Two DOF mechanism in thumb design.

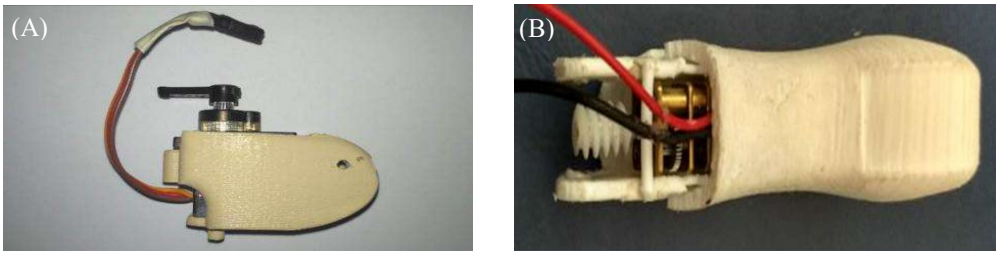

Figure 10 Actuator placement in the thumb (A) opposition/reposition, (B) flexion/extension.

2.2 Myoelectric hardware and software system

A surface Electromyography (sEMG) sensor was used to read the muscle activity in the remaining hand of the amputee. The EMG sensor from RSL steeper shown in Figure 11 was selected in this research due to its state-of-the-art nature with outstanding capture and amplification as well as some features such as the superior sensitivity to capture a low muscle signal, proportional control, and built-in gain adjustment. Moreover, the interference protection used for the myoelectric hand is 50 Hz. The raw signal of the EMG was processed using signal processing techniques such as amplification and rectification while the sensor was powered from 5 V to 19 V. The technical specification of the EMG sensor summarized in Table III showed it has a small size and light-weight which makes its placement in the socket of the myoelectric hand to be easy.

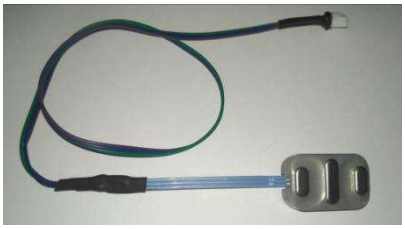

Figure 11 The electromyography used in the myoelectric hand.

Table 3 Specification of the Bebionic EMG electrode.

Parameter	Values
Dimension (L x W x H)	27x18x10 mm
Mass	4.4 gr
DC power supply	5-19 V
Frequency range	90 to 450 Hz
Temperature range	-15 to 60 °C
Max relative humidity	95 %

The EMG sensor is worn on the healthy normal hand of the participant, attached to the flexor carpi radialis, and placed below the elbow as shown in Figure 12 after which the participant was asked to perform hand flexion and extension. The output signal was acquired using the Arduino Mega microcontroller with serial communication via USB, processed with a sampling frequency of 50 Hz, and filtered with a first-order low-pass filter as expressed in Equation (18). The scale of gain on EMG is obtainable from one to six but four was used in this research. The filtered EMG signal was finally used to capture the motion of the user's hand as depicted in Figure 13. The results showed it smooth enough and can be used as a signal command to drive the motion of the servo motor angle in the fingers.

$$G(\mathrm{s}) = \frac{1}{0.2s + 1} \tag{18}$$

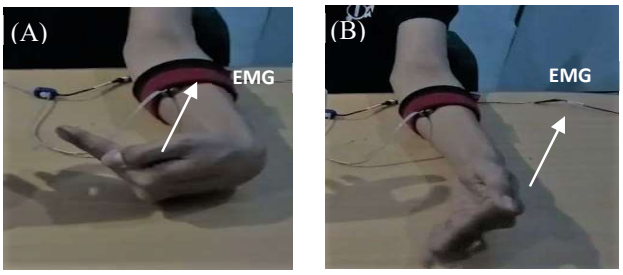

Figure 12 EMG sensor placement and acquisition (A) Flexion (B) Extension.

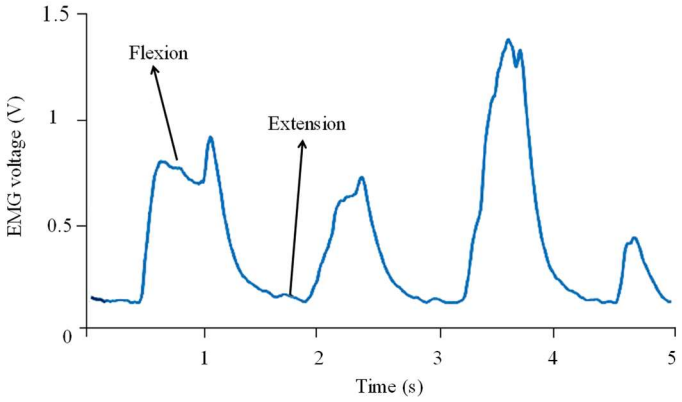

Figure 13 Filtered EMG signal from a healthy study participant.

The proposed myoelectric hand which was named "BimoHand" has six grip patterns which include power grasp, key grasp, pinch, tripod, active index, and hook. These selected patterns have been reported in previous studies [1,2,20,21] to be widely used in the activity of daily living [ADL]. A tactile switch was also employed to select the desired grip pattern while the signal presented in Figure 13 was used to drive the motion of the fingers. The current working of the selected grip is indicated with the sequence of on-off LED and the operating system used in controlling the finger motion is presented in Figure 14.

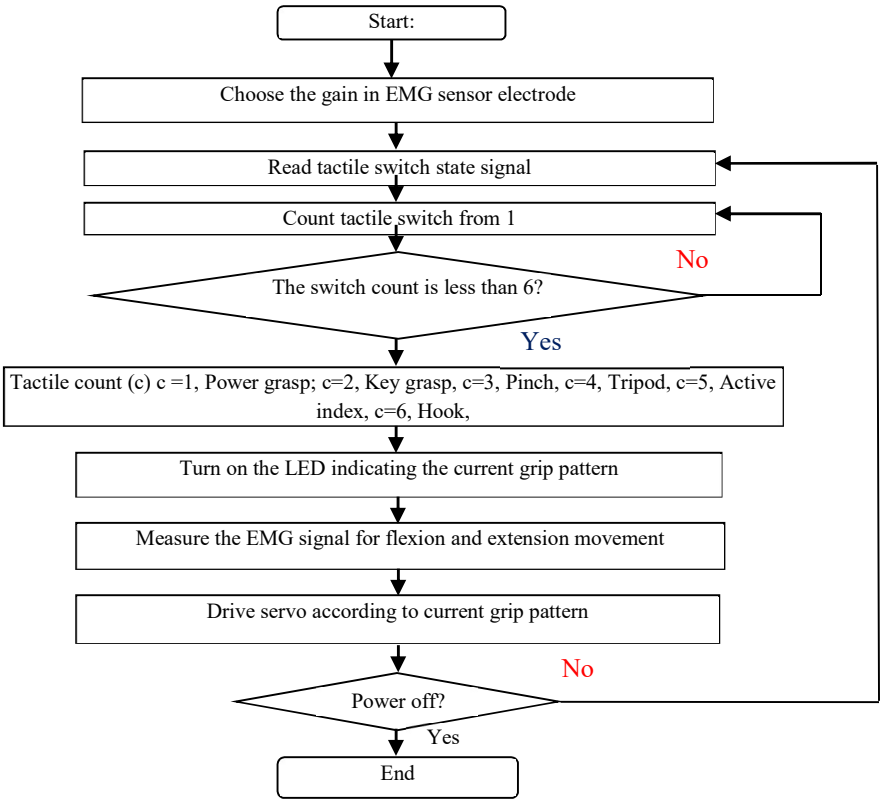

Figure 14 Flowchart of the BimoHand operation system.

The operating system was developed in MATLAB/Simulink environment and the algorithm was embedded into an Arduino Nano. The controller has a small size 8-bit microcontroller which is suitable for the BimoHand due to its size and weight. The Arduino Nano also has 14 digital input-output (DIO) pins and 8 analog input pins which are considered enough to interface the sensors and actuator in the hand.

3. Results and discussion

This section presents the trajectory of points in two six-bar linkages and the six designed grip patterns tested using EMG signals through the use of a participant with a healthy hand. This involved testing the hand by grasping objects with different sizes, shapes, and weights as well as fragile objects such as an egg without force feedback closed-loop control. Meanwhile, the force in each finger was measured using a force-sensitive resistor (FSR).

3.1 Finger kinematics

The kinematics results for the six-bar linkages presented in Figure 4 are divided into two six-bar loops which include O_1ABO_2, and O_2O_3CD. The two linkages were used in the index, middle, ring, and little fingers while the length and range of motion of each link in loop O_1ABO_2 are shown in Table I. The input angle θ was found to be 65^0-125^0, 20^0-110^0, 5^0-85^0, 5^0-85^0 in index, middle, ring, and little fingers respectively as directly measured from the proposed myoelectric BimoHand. Moreover, the trajectory of point A and point B depicted in Figure 15 shows the middle finger has the shortest diameter because the link AO_1 has the shortest length.

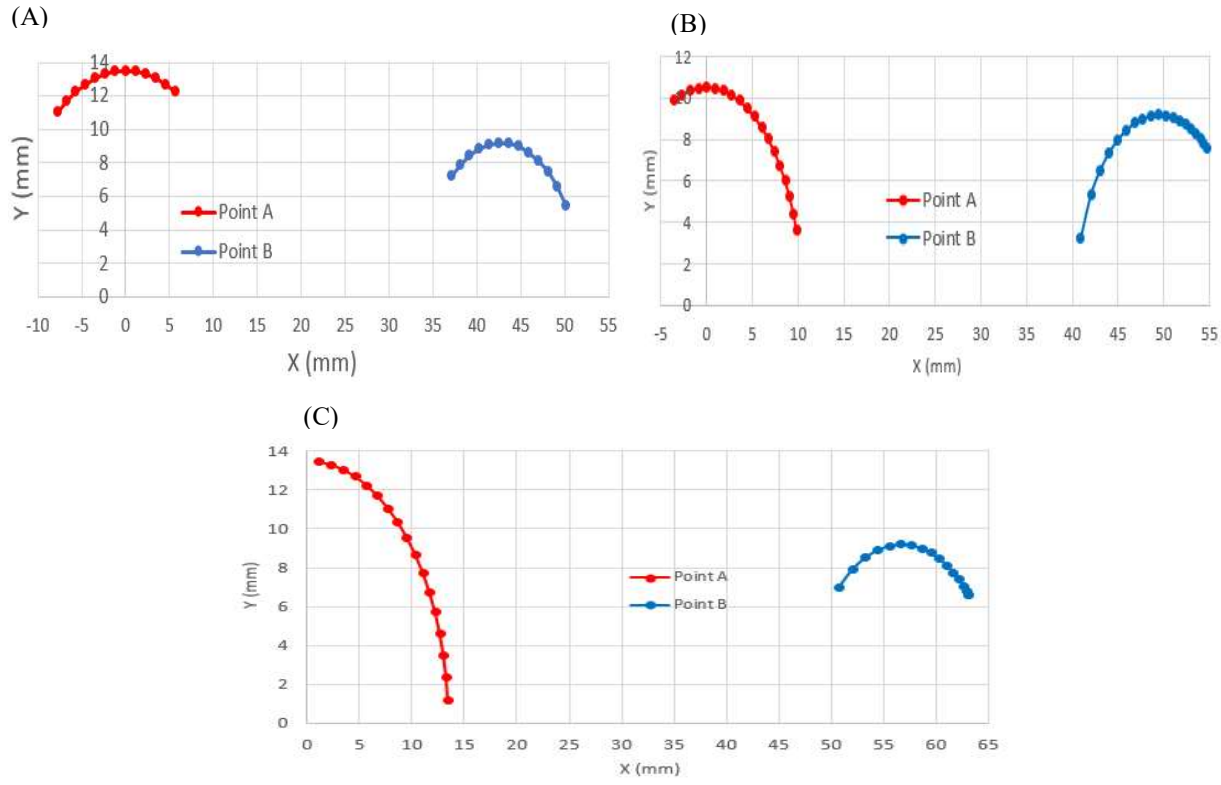

Figure 15 Trajectory of point A and B (A) index finger linkage, (B) middle finger linkage (C), ring and little finger linkage.

The kinematics results of the cross six-bar linkage for O_2O_3CD are shown in Figure 16 and the link parameters summarized in Table II were used to calculate the trajectory of link O_2D and DE using Equations (12) to (17). Moreover, the angle γ for the index, middle, ring, and little fingers used in this model has a value ranging from 0^0 to 90^0 while β was from 9.71^0 to 113.64^0. The simulation for the finger workspace showed all the four fingers have a similar pattern with a human hand and these results were used to propose the two four-bar linkages applied as the mechanism for the myoelectric prosthetic hand.

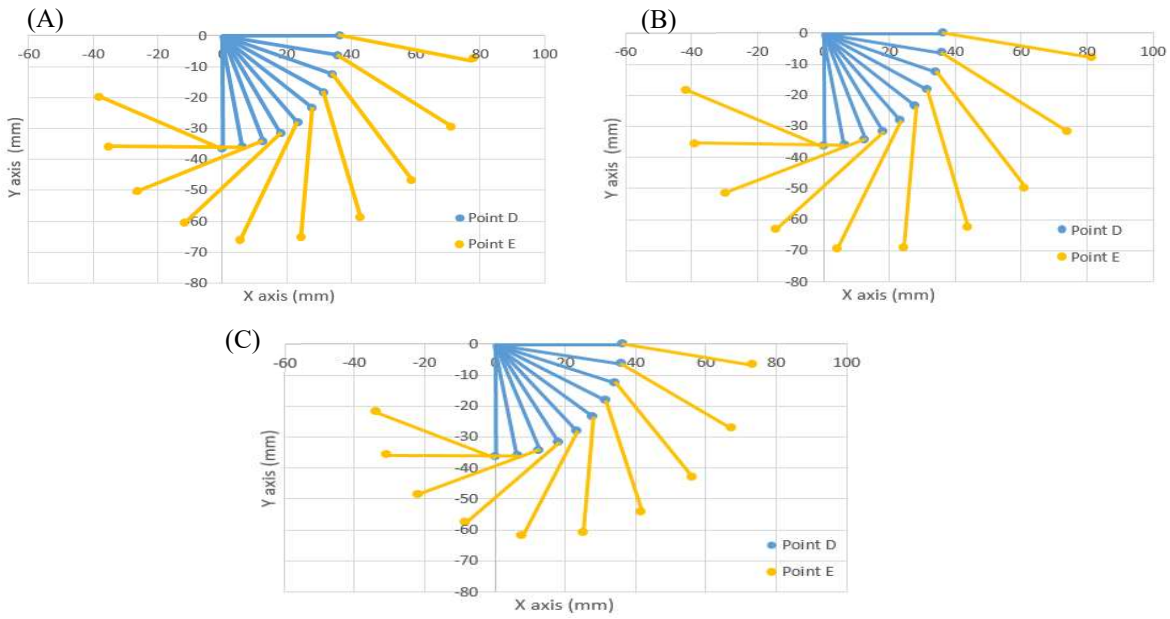

Figure 16 Finger trajectories (A) index and ring finger workspace (B) middle finger workspace (C) Ring finger workspace.

3.2 Grasping test

The myoelectric hand was tested for six different grip pattern modes and the command signal from the sEMG sensor was found to be the same for hand extension and flexion as shown in Figure 13. This signal command was acquired from a subject with a healthy hand and the results presented in Figure 17 showed the myoelectric hand designed was able to perform all the modes successfully.

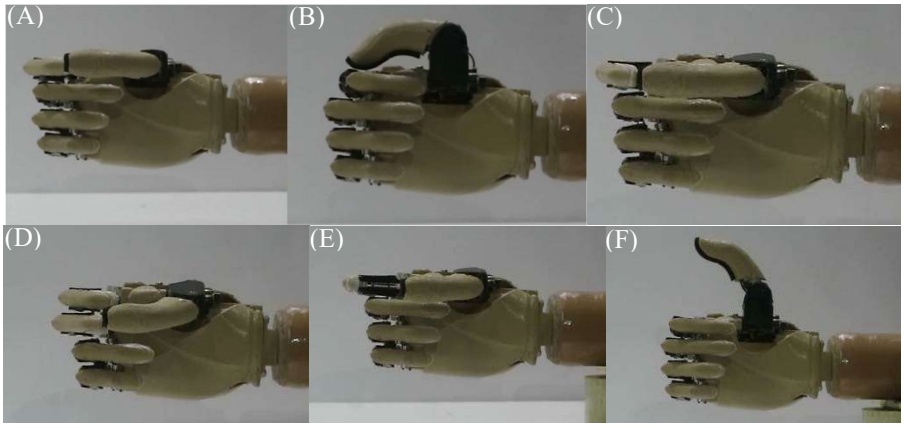

Figure 17 Six grip pattern modes from the proposed hand (A) Power grasp, (B) Key grasp, (C) Pinch, (D) Tripod, (E) Active index, (F) Hook.

The hand was also used to grip 21 several objects as shown in Figure 18. This involved using the healthy hand of a study participant to drive the hand towards grasping and picking small objects such as coins, flash disk, nut, name card, and a paper clip. It is important to note that the pinch grip mode is widely used in precision object grasping, especially for small objects. The power grasp is for objects such as a bottle with drinking water using the maximum force available in the hand. The tripod mode is to pick and grasp objects such as screwdriver, ballpoint, and spoon while the key grasp mode is for an object like a key. Moreover, the hook grip mode is for an object like a headphone while the active index mode was designed to type on the keyboard. The grasping performances of the proposed myoelectric BimoHand is presented online at https://www.youtube.com/watch?v=VXv4pu6ynTY.

Figure 18 Grasping test using different objects.

The individual forces in the fingers of the proposed hand were also measured using a calibrated force-sensitive resistor (FSR) which was placed on the fingertip when a finger is in the rest position as shown in Figure 19. The servo motor in each finger was commanded to close at full power from 0^0 to 180^0. The values of the forces presented in Figure 20 showed a linear relationship between the force of each finger and the servo angle input with the index finger recorded to have the highest value.

Figure 19 Grip force measurement using the FSR sensor.

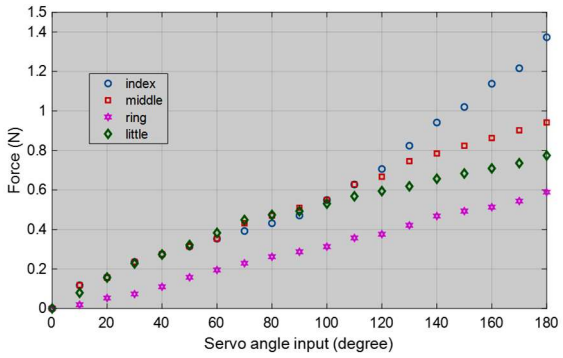

Figure 20 Individual forces at fingertip based on the servo angle input.

The grip force generated by each fingertip was influenced by the length of the link from the servo motor to the fingertip and the servo motor torque. This is based on the principle that force is directly proportional to the torque and inversely proportional to the length of the link in each finger. Meanwhile, the maximum forces in each finger are presented in Figure 21 while the servo motor torque and link length are summarized in Table IV. The actuator servo motors of the index and middle fingers have individual torque of 2.5 kg.cm while the ring and little fingers have a joint link from a single servo motor with 1.25 kg.cm torque.

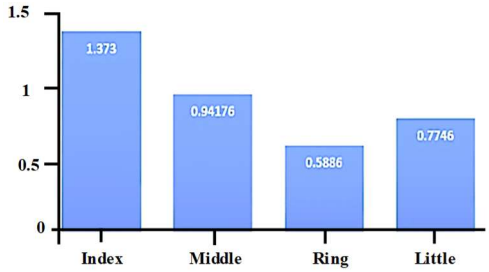

Figure 21 Maximum force (N) for each finger.

Table 4 Torque and link length of the finger.

Finger	Link length in middle-distal (mm)	Motor torque (kg.cm)
Index	43	2.5
Middle	50	2.5
Ring	43	1.25
Little	34	1.25

The individual grip force at the fingertip in the proposed BimoHand ranged from 0.5886 N to 1.373 N and this is relatively low compared to other commercially available myoelectric prosthetic hands such as Vincent, iLimb, and Bebionic. For example, the values for Belter [19] and Vincent large hand were found to be between 4.82 N and 8.44 N, iLimb has from 3.09 N to 11.18 N while Bebionic has the highest which ranges from 12.25 N to 16.11 N.

The prototype produced has a size similar to the average Asian human hand as shown in Figure 22 while its general specification is summarized in Table V. The hand can only be used to pick and grasp an object with a maximum weight of 1.5 kg due to its low grip force generated at the fingertip in comparison with the high-end commercial myoelectric hand. It also has very lightweight with a total mass of 251 gram excluding socket and batteries and this is in line with the findings of Balter [19] that a myoelectric hand needs to be below 500 grams to avoid user fatigue.

The maximum individual grip force generated in each finger was relatively low and this makes the hand to be perfect in grasping fragile objects without force feedback control. This was observed from the test conducted to grasp an egg without force feedback control with the closure of the fingers controlled using one channel EMG sensor through the use of a healthy hand. Meanwhile, the human hand attached with the EMG sensor was able to adjust the muscle activity for flexion and extension with the opening or closing of the prosthetic hand to control the strength of the grip. Figure 23 shows the healthy human hand was able to successfully control the grip of the prosthetic hand without breaking the egg.

Figure 22 The proposed BimoHand shakes hand with a human hand.

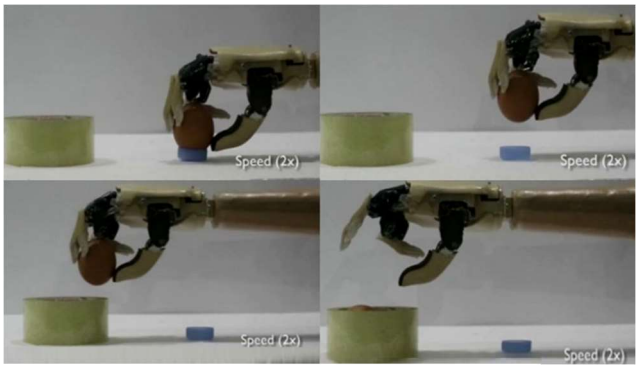

Figure 23 Sequence images of the hand grasping an egg.

3.3. Comparison with other affordable myoelectric hands

An affordable myoelectric hand can be achieved using 3D printer technology to have a fairly lightweight product. The cost of the previous AstoHand [2] excluding labor and production was estimated at 1500 USD while some other open-source produced using 3D printers include Tact, Ada, and Dextrus as well as the HACKberry from Japan which costs approximately 160,000 JPY. Another affordable myoelectric hand produced from a 3D printer is Touch hand which was developed by the University of KwaZulu-Natal, Durban,

South Africa, and valued to be 1,052 USD including labor and electricity which is 40 times lesser than the available commercial hands on the market [22]. Meanwhile, the affordable hands based on 3D printers as well as the commercially available high-end products are summarized in Table 5.

The price of high-end products available in markets varies from 10,000 USD to 100,000 USD with a Bebionic hand from Otto Bock considered to be the best with a grip force up to 45 kg as well as the application of gears and leadscrews in driving each finger. The other expensive products are Vincent hand, Michelangelo hand, and iLimb.

An affordable myoelectric hand was successfully developed in this study based on 3D printer technology. It is driven by three micro servo motors and one DC motor and has six grip patterns including power grasp, key grasp, pinch, tripod, active index, and hook. The hand also has a lightweight of 251 g due to the presence of Polylactic acid (PLA) while the weight of the battery and hand socket is 195 g which makes the total weight to be 446 g. One complete grip pattern mode which is the time to close and open the hand is also just 1.5 sec and the total cost is less than 500 USD excluding the sensor and socket as shown in the general specification presented in Table 6. Meanwhile, one of the disadvantages of this hand, when compared to other bionic hands on the market, is that its weight limit is 1,500 g.

Table 5 Comparison with other available myoelectric hands.

Hand	Developer	Mass (hand)	Size (length x width x thickness, mm)	Numb. of Joint	DOF	Numb. Of Actua-tor	Motor Actuator Type	Joint couple method
Asto Hand v2 (2016) [2]	Diponegoro University	430	180 x 85 x 50	10	5	5	Lead Screw motor	Tendon -spring
Tact (2015) [3]	University of Illinois	350	200 x 98 x 27	11	6	6	Ten-don DC motor	Linkage
Rehand (2015) [4]	NAIST, Japan	467	Human hand size	14	1	1	Lead Screw motor	Linkage
Keio Hand (2008) [7]	Keio University	730	320 mm length 120 mm fingers	15	15	1	Ultra-sonic motor	Single tendon for each finger
Ada Hand (2016) [8]	Open Bionics	380	215x 178 x 58	10	5	5	Lead screw	Tendon
Dextrus (2013) [9]	Open Hand Project	428	205 x 88 x 45	15	6	6	Tendon DC motor	Tendon
HACKberry hand [10,21]	exiii Inc.	-	-	10	6	3	Servomotor	Linkage
Vincent Hand (2010) [11]	Vincent system	-	-	11	6	6	Worm gear motor	Linkage
Michelangelo (2012) [12]	Otto Bock	420	-	6	2	2	-	Cam design to all finger
Bebionic (2011) [13,20]	RSL Steeper	495-539	198 x 90 x 50	11	6	5	Lead Screw motor	Lingkage
Bebionic v2 (2011) [13,20]	RSL Steeper	495-539	190-200 x 84-92 x 50	11	6	5	Lead Screw motor	Lingkage
iLimb (2009) [14,20]	Touch bionic	450-615	180-182 x 75-80 x 35-41	11	6	5	Worm gear motor	Tendon
iLimb Pulse (2010) [14,20]	Touch bionic	460-465	180-182 x 75-80 x 35-45	11	6	5	Worm gear motor	Tendon
Touch Hand II [22]	University of KwaZulu	451	-	14	6	6	Tendon-DC motor	Tendon-pulley

Table 6 General specification of the developed myoelectric hand.

Body material	Polylactic acid (PLA)	
Linkage material	Acrylic	
Number of fingers	4 fingers & a thumb	
Number of actuators	3 servo motors and 1 DC motor	
Number of joints	10 joints (two in each finger)	
Number of patterns	6 grip patterns (power grasp, Key grasp, Pinch, Tripod, Active index, Hook)	
Actuator	Fingers	Servo motor
	Thumb	Servo and DC motor
Total weight	251 g	
Maximum load	0.3 kg for each finger	
Electromyography	EMG from RSL Steeper BeBionic	
Battery	Type	Polymer Lithium-Ion Battery
	Numb. of batteries	2 x (18650 Li-Ion batteries)
	Voltage	3.7 V
	Capacity	2600 mAh
Time for closing to opening	1.5 s	
Communication	Serial communication (USB)	

The motion of the fingers for flexion and extension can be controlled directly using sEMG based on the ability of the microcontroller on the hand to read the voltage level from an onboard signal processing circuit in the sEMG using an analog-to-digital (ADC) pin as shown in Figure 13. Meanwhile, the feature extraction and machine learning techniques were not required to process this output voltage signal but a low-pass filter was applied to filter its high frequency to make it smoother. The voltage varies from 0 V for full hand extension to 1.5 V for full hand flexion and was converted to the desired angle for the servo motor through the implementation of constant gain in the system. However, the maximum angle required for the servo motor to drive the finger is 900 and it is possible for the wearer or user to adjust the motion of the finger directly by moving the hand flexion/extension based on the sEMG signal conversion. The video showing the BimoHand performance during the grasping tests for several objects is accessible on YouTube at https://bit.ly/37zmO3J while its performance when it was worn by trans-radial amputees is at https://bit.ly/3h77hex.

4. Conclusion

A low-cost myoelectric prosthetic hand was designed using a six-bar linkage and developed through the use of a 3D printer. The product has a mass of 251 grams and the same size as an average Asian human hand. This weight is discovered to be efficient for people with below elbow amputation due to their need for a lighter myoelectric prosthetic hand for the activity of daily living. Moreover, the total cost of the material is less than 500 USD excluding the sensor and socket. The hand has the ability to pick and grasp several objects with a maximum weight of 1.5 kg based on six grip patterns and the grasping test also showed it is efficient for people with trans-radial/below elbow amputation in performing ADL. Meanwhile, the individual grip force for each finger was observed to be relatively low compared to a commercially available high-end prosthetic hand and this means it has the ability to successfully pick and grasp an egg without breaking it by adjusting the human hand flexion and extension.

There is, however, the need to use high torque servo motor with metal gear to increase the individual grip force for each finger in future research work, and the grasping control algorithm is required to be developed using artificial intelligence. Moreover, the proposed myoelectric prosthesis will be implemented on study participants with a trans-radial amputation.

5. Acknowledgments

This research was funded by Diponegoro University (Undip) under the Riset Unggulan UNDIP (RUU) from the PNBP DIPA Universitas Diponegoro with contract No: SP DIPA-042.01.2.400898/2016.

6. References

[1] Ariyanto M, Haryadi GD, Ismail R, Pakpahan JA, Mustaqim KA. A low-cost anthropomorphic prosthetic hand using DC micro metal gear motor. In: Facta M, Riyadi MA, Widianto ED, Arfan M, editors. 2016 3rd International conference on information technology, computer and electrical engineering (ICITACEE); 2016 Oct 19-20; Semarang, Indonesia. IEEE; 2016. p. 42-46.

[2] Ariyanto M, Ismail R, Mustaqim KA, Putri FT, Setiawan JD, Sumarwoto T. An affordable myoelectric hand augmented with 3D virtual hand for transradial prosthesis. Int J Mech Mechatron Eng. 2017;17(06):86-96.
[3] Slade P, Akhtar A, Nguyen M, Bretl T. Tact: design and performance of an open-source, affordable, myoelectric prosthetic hand. In: Okamura A, Antonelli G, Burschka D, editors. 2015 IEEE International conference on robotics and automation (ICRA); 2015 May 26-30; Seattle, USA. IEEE; 2015. p. 6451-6456.
[4] Yoshikawa M, Sato R, Higashihara T, Ogasawara T, Kawashima T. Rehand: realistic electric prosthetic hand created with a 3D printer. In: Cerutti S, Bonato P, Lovell N, Mainardi C, editors. 2015 37th annual international conference of the IEEE engineering in medicine and biology society (EMBC); 2015 Aug 25-29; Milan, Italy. IEEE; 2015. p. 2470-2473.
[5] Cipriani C, Controzzi M, Carrozza MC. Objectives, criteria and methods for the design of the smarthand transradial prosthesis. Robotica. 2010;28(6):919-927.
[6] Controzzi M, Cipriani C, Carrozza MC. Mechatronic design of a transradial cybernetic hand. In: Chatila R, Merlet J, Laugier C, editors. 2008 IEEE/RSJ International conference on intelligent robots and systems; 2008 Sep 22-26; Nice, France. IEEE: 2008. p. 576-581.
[7] Kamikawa Y, Maeno T, Underactuated five-finger prosthetic hand inspired by grasping force distribution of humans. In: Chtila R, Merlet J, Laugier C, editors. 2008 IEEE/RSJ international conference on intelligent robots and systems; 2008 Sep 22-26; Nice, France. IEEE: 2008, p. 717-22.
[8] Raines J, Robotics Hand Development Kit-Ada V1.1 -Datasheet, United Kingdom, Open Bionics, May 2016.
[9] Openhandproject.org [Internet]. Bristol: The Organization; c2013 [cited 23 May 2020]. Available form: http://www.openhandproject.org/.
[10] Koprnický J, Najman P, Šafka J. 3D printed bionic prosthetic hands. In: Capmany J, editor. IEEE International workshop of electronics, control, measurement, signals and their application to mechatronics (ECMSM); 2017 May 24-26; Donostia, Sebastian. València: IEEE; 1963. p. 1-6.
[11] Vincentsystems.de [Internet]. Karlsruhe: Company Limited; c1998 [cited 24 May 2020]. Available form: https://www.vincentsystems.de/?lang=en.
[12] Ottobockus.com [Internet]. Texas: The Organization; c2015 [cited 24 May 2020]. Michelangelo prosthetic hand. Available form: https://www.ottobockus.com/prosthetics/upper-limb-prosthetics/solution-overview/michelangelo-prosthetic-hand/.
[13] Ottobockus.com [Internet]. Texas: The Organization; c2015 [cited 24 May 2020]. Bebionic-hand. Available form: https://www.ottobockus.com/prosthetics/upper-limb-prosthetics/solution-overview/bebionic-hand/.
[14] Össur Co., Ltd [Internet]. Reykjavík: Company Limited; c1971 [cited 24 May 2020]. i-Limb® Access. Available form: https://www.ossur.com/en-gb/prosthetics/arms/i-limb-access.
[15] Jeong SH, Kim KS, Kim S. Designing anthropomorphic robot hand with active dual-mode twisted string actuation mechanism and tiny tension sensor. IEEE Robot Autom Lett. 2017;2(3):1571-1578.
[16] Tavakoli M, Batista R, Sgrigna L. The UC softhand: light weight adaptive bionic hand with a compact twisted string actuation system. Actuators 2016;5(1):1.
[17] Hosseini M, Meattini R, Palli G, Melchiorri C. A wearable robotic device based on twisted string actuation for rehabilitation and assistive applications. J Robot. 2017;2017(1):1-11.
[18] Guo G, Zhang J, Gruver W. Optimal design of a six-bar linkage with one degree of freedom for an anthropomorphic three-jointed finger mechanism. J Eng Med.1993;207:185.
[19] Shen JQ, Russell K, Sodhi RS. On function generation of watt I mechanisms for finger design. In: Gezgin E, Akgün Y, editors. International symposium of mechanism and machine science (ISMMS); 2010 Oct 5-8, Izmir, Turkey. New York: Curran Associates, Inc; 2002. p. 411-422.
[20] Belter JT, Segil JL, Dollar AM, Weir RF. Mechanical design and performance specifications of anthropomorphic prosthetic hands: a review. J Rehabil Res Dev. 2013;50(5):599-618.
[21] Exiii-hackberry.com [Internet]. Tokyo: Incorporation; c2014 [cited 25 May 2020]. Available form: http://exiii-hackberry.com/.
[22] Jones GK, Stopforth R. Mechanical design and development of the touch hand ii prosthetic hand. R&D J. 2016;(32):23-34.